An Experimental and Mechanistic Investigation of the Complexities Arising During Inhibition of the *Briggs–Rauscher* Reaction by Antioxidants

by **Rinaldo Cervellati***[a]), **Kerstin Höner**[b]), **Stanley D. Furrow**[c]), **Francesco Mazzanti**[a]), and **Stefano Costa**[a])

[a]) Dipartimento di Chimica 'G. Ciamician', Università di Bologna, Via Selmi, 2, I-40126 Bologna (phone: +390512099467; fax: +390512099456; e-mail: rinaldo.cervellati@unibo.it)

[b]) Institut für Fachdidaktik der Naturwissenschaften, Abt. Chemie und Chemiedidaktik, Technische Universität Braunschweig, Pockelsstrasse 11, D-38106 Braunschweig

[c]) Penn State University, Berks-Lehigh Valley College, Luerssen Building, PO 7009, Reading, PA 19610-6009, USA

A method to determine the relative antioxidant capacity of radical scavengers based on the inhibition of the oscillations of the *Briggs–Rauscher* (*BR*) oscillating reaction was previously reported. A semiquantitative mechanistic interpretation of the inhibitory effects required two steps to obtain simulated inhibition times in very good agreement with the experimental ones. The first step is inhibitory, involving H-atom transfer from antioxidant to the HOO• radical; the second step is a first-order degradation of the antioxidant to unspecified products. Since the degradation may be due to oxidation and/or iodination of the antioxidant, we studied the kinetics of the subsystems $IO_3^-(H^+)$ + antioxidant and $I_2(H^+)$ + antioxidant. We used 2,5- and 2,6-dihydroxybenzoic acids, caffeic acid (= 3-(3,4-dihydroxyphenyl)prop-2-enoic acid), ferulic acid (= 3-(4-hydroxy-3-methoxyphenyl)prop-2-enoic acid), pyrocatechol (= benzene-1,2-diol), and hydroquinone (= benzene-1,4-diol) as antioxidants. Spectra in the wavelength range 500–250 nm were repeated at given time intervals to follow the peaks of the iodine and oxidation products, which were mainly quinones. For the iodination of the above diphenols (= benzenediol derivatives) the substitution and/or addition reactions with I_2 or HOI were found to be relatively slow compared to oxidation by IO_3^-. Approximate rate constants for oxidation were obtained on the basis of a reasonable kinetic model by using a suitable numerical integration program. Although these complexities can arise also in the completely inhibited *BR* oscillator, we believe that the inhibitory effects are due to the HOO• scavenging action by diphenols or by quinones since HOO• radicals are also potential reducing agents. We propose two steps that could maintain a small reservoir of diphenol, while both quinone and diphenol deplete HOO• radicals. In short, the complexities do not affect the method for monitoring the relative activity of antioxidants based on the *BR* oscillating reaction. The effects of temperature on the inverse of the oscillatory time in the *BR*-uninhibited system, on the inverse of inhibition times, and on the time length of the resumed oscillations for four antioxidants were also investigated. Apparent average activation energies were obtained.

1. Introduction. – A new method for the measurement of antioxidative activity recently reported [1] is based on the inhibitory effects by antioxidants on the oscillations of the hydrogen peroxide, acidic iodate, malonic acid, Mn^{II}-catalyzed system, known as the *Briggs – Rauscher* (*BR*) reaction [2]. The inhibitory effect of antioxidants added to an active oscillating *BR* mixture consists of an immediate cessation of oscillations, an inhibition time that linearly depends on the concentration of the antioxidant added in a wide range of concentration, and subsequent regeneration of oscillations, as shown in *Fig. 1*. The latter shows a representative trace of the bright Pt-electrode potential *vs.* time for a reference oscillator and an inhibited oscillator. The oscillatory time in the uninhibited system is shown in *Fig. 1*, *a*, and the moment of antioxidant addition, the inhibition time, and the time length of resumed oscillations

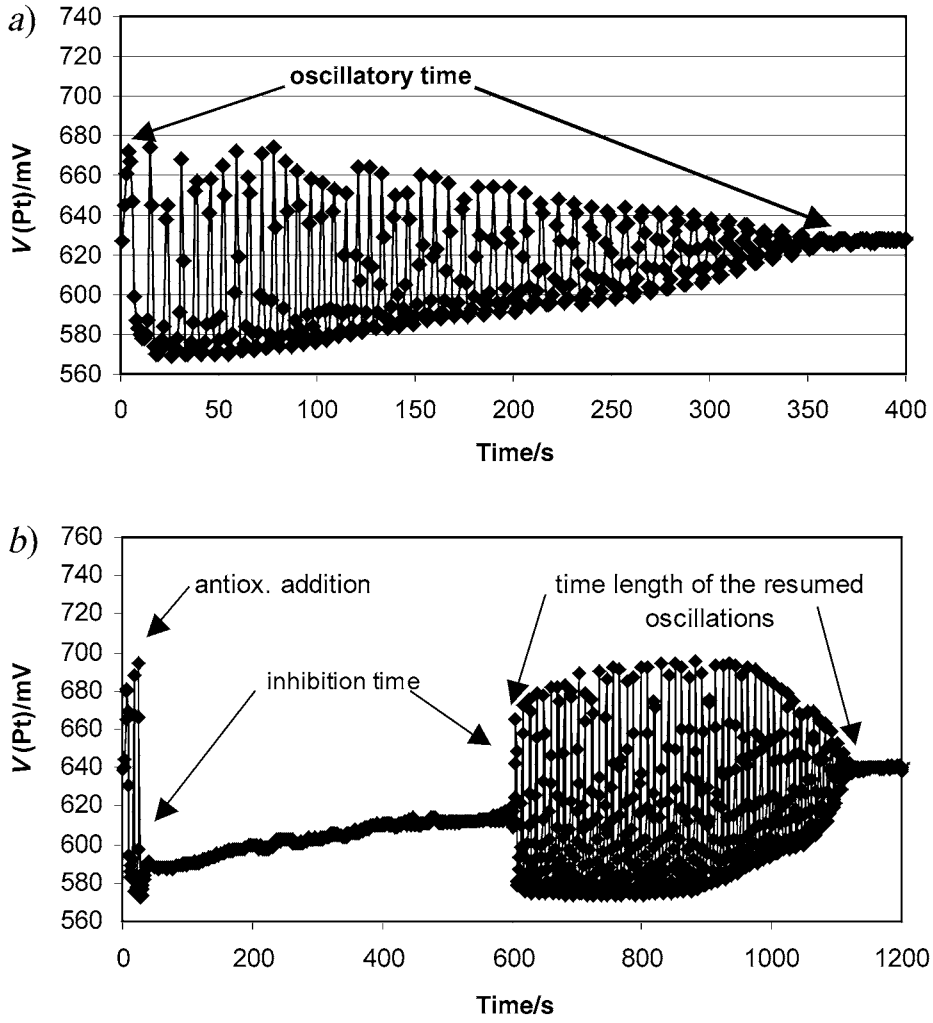

Fig. 1. a) *Uninhibited* BR *reaction: recording of the potential of the solution* vs. *time of an oscillating* BR *mixture* (initial conditions: $[H_2O_2] = 1.5$M, $[HClO_4] = 0.0334$M, $[IO_3^-] = 0.0667$M, [malonic acid] = 0.050M, $[Mn^{2+}] = 0.0063$M). b) *Inhibited reaction: recording of the potential of the solution* vs. *time when 1 ml of a solution of caffeic acid* (0.03 mg/ml) *was added to 30 ml of an oscillating* BR *mixture after the third oscillation* (initial conditions: the same as in *Fig. 1,a*).

are shown in *Fig. 1,b*. The method was validated on ten substituted diphenols (= benzenediol derivatives; $Ar(OH)_2$) [1] and was successfully tested on sixteen German white wines [3], fruit and vegetable extracts [4], and natural polyphenolic compounds [5].

The main intermediates for which concentrations oscillate in the *BR* reaction are I_2, I^- ion, the oxyiodine species HOI, HOIO, and $IO_2^{\bullet}$, and the hydroperoxyl radical $HOO^{\bullet}$. The involvement and important role played by $HOO^{\bullet}$ radicals in the onset of

oscillations has been recognized in previous work [6][7]. We have ascribed inhibitory effects to the antioxidants' scavenging action against HOO· radicals [1][6].

Very recently, *Furrow et al.* [7] reported a new mechanism for the *BR* reaction that takes into account the important role played by HOO· radicals in its oscillatory behavior. With this new mechanism, now referred to as the *FCA* model, *Furrow et al.* [7] obtained not only better agreement between experimental results and simulations for malonic acid and its derivatives with respect to a previous mechanism [8], but the *FCA* model is able to simulate oscillations in *BR* systems with substrates that are iodinated in a different way than malonyl derivatives, such as crotonic and acrylic acids (=(2*E*)-but-2-enoic and prop-2-enoic acids, resp.), anisole (PhOMe), and 4-nitrophenol [7].

To try to simulate the inhibitory effects of an antioxidant on the oscillations, the step of *Eqn. 1* was added to the *FCA* model, where $Ar(OH)_2$ indicates a generic diphenol[1]). Caffeic acid (= 3-(3,4-dihydroxyphenyl)prop-2-enoic acid; CA) was chosen for the simulations [1]. With minor changes, rate constants used in the simulations were those reported in [7]. The inhibitory step was added and allowed to vary for the best fit with the experimental behavior. With just this step, the inhibition time is very sensitive to the amount of inhibitor (roughly, increasing the inhibitor by 10% leads to an increase in inhibition time of nearly 50%) [1]. Thus, we added a second step, *i.e.*, first-order degradation of the inhibitor to unspecified products (*Eqn. 2*).

$$IN \qquad Ar(OH)_2 + HOO^{\cdot} \rightarrow Ar(OH)O^{\cdot} + H_2O_2 \quad (Ar(OH)O^{\cdot} \text{ decays to products}) \tag{1}$$

$$DEG \quad ArO-H \rightarrow \text{products} \tag{2}$$

The degradation may be due, *e.g.*, to oxidation and/or iodination of ArOH. With this additional step, we obtained very good agreement between the experimental and calculated inhibition time for caffeic acid (see Fig. 9 of [1]). The same agreement was obtained with different initial caffeic acid concentrations. The simulations are based on the *FCA* model [7], reproduced in *Table 1* with addition of the steps *IN* and *DEG*. References for the rate constants are given in [7], except for k_{C3}, k_{C3R}, and k_{C4} [8]. The species on the left, not in parentheses, are those included in the rate laws. Water is used with an activity of 1. Even though it is not permissible to compare rate constants from different-order rate equations, k_{IN} for caffeic acid is several orders of magnitude higher than k_{DEG}, so we concluded that in any case, the scavenging action by the diphenols against HOO· radicals is the source of the inhibition of oscillations [1].

The main goal of this paper is a more-detailed study of the complexities that could arise in the inhibitory effects by antioxidants on the *BR* reaction. Since the antioxidants can react with other components in the *BR* mixture, the *DEG* step must be a composite of several parallel reactions. Preliminary work showed that the most-important side reactions were oxidation and iodination of diphenolic species by iodate (IO_3^-), I_2, or HOI. Some qualitative evidence has been reported in [1].

Another goal is to investigate the dependence of the inhibition time and of the time length of the resumed oscillatory phase on the temperature. Preliminary experiments

---

[1]) In [1], the step *IN* was reported as $ArO-H + HOO^{\cdot} \rightarrow ArO^{\cdot} + H_2O_2$; both terminologies refer to the same process.

Table 1. *The* FCA *Model* [7] *with Addition of Steps* IN *and* DEG

Step	Reaction	Rate constant
I1	$HOI + I^- \rightarrow I_2 + H_2O - H^+$	$3.67 \cdot 10^9$ M^{-1} s^{-1}
I1R	$I_2 (+ H_2O) - H^+ \rightarrow HOI + I^-$	$1.98 \cdot 10^{-3}$ s^{-1}
I2	$I^- + HOIO \rightarrow 2\,HOI - H^+$	$5.0 \cdot 10^9$ M^{-1} s^{-1}
I3	$I^- + IO_3^- + 2\,H^+ \rightarrow HOI + HOIO$	$1.43 \cdot 10^3$ M^{-3} s^{-1}
I5R	$2\,IO_2^{\bullet} (+ H_2O) \rightarrow HOIO + H^+ + IO_3^-$	$5.0 \cdot 10^9$ M^{-1} s^{-1}
M	$HOIO + H_2O_2 + Mn^{2+} (+ H_2O_2) \rightarrow 2\,HOO^{\bullet} + Mn^{2+} + H_2O$	$3.1 \cdot 10^4$ M^{-2} s^{-1}
D2	$H^+ + IO_3^- + HOO^{\bullet} \rightarrow IO_2^{\bullet} + H_2O + O_2$	$1.3 \cdot 10^4$ M^{-2} s^{-1}
D3	$IO_2^{\bullet} + H_2O_2 \rightarrow HOIO + HOO^{\bullet}$	$2.0 \cdot 10$ M^{-1} s^{-1}
D1	$HOI + H_2O \rightarrow I^- + O_2 + H^+ + H_2O$	5 M^{-1} s^{-1}
O2	$2\,HOO^{\bullet} \rightarrow H_2O_2 + O_2$	$7.5 \cdot 10^5$ M^{-1} s^{-1}
C3	$CH_2(COOH)_2$ (diacid) $\rightarrow$ (HOOC)CH=C(OH)$_2$ (enol)	$3.9 \cdot 10^{-3}$ s^{-1}
C3R	(HOOC)CH=C(OH)$_2$ (enol) $\rightarrow$ $CH_2(COOH)_2$ (diacid)	$9.1 \cdot 10$ s^{-1}
C4	(HOOC)CH=C(OH)$_2$ (enol) $+ I_2 \rightarrow$ ICH(COOH)$_2$ (diacid) $+ I^- + H^+$	$9.1 \cdot 10^5$ s^{-1}
IN	$Ar(OH)_2 + HOO^{\bullet} \rightarrow Ar(OH)O^{\bullet} + H_2O_2$	see *Table 2*
DEG	$Ar(OH)_2 \rightarrow$ products	see *Table 2*

have shown that the dependence of the oscillatory time in an uninhibited mixture on the temperature approximates *Arrhenius*-type behavior. A plot of log(1/oscillatory time) *vs.* $(1/T)$ yields a straight line, so from its slope an apparent 'activation energy' can be found. A comparison of this apparent 'activation energy' with those obtained for the inhibition phase and the resumed oscillations phase could definitely establish the different features occurring during these phases.

2. Experimental. – Malonic acid (*Merck*, reagent grade, >99%), manganese(II) sulfate monohydrate (*Merck*; reagent grade, >99%), $NaIO_3$ (*Merck*; reagent grade, >99.5%) were used without further purification. $HClO_4$ (*Merck*; 70–72%), H_2O_2 (*Merck*; 35–36.5%), and other chemicals were of anal. grade. Perchloric acid was analyzed by titration *vs.* a standard 0.1M NaOH soln. (from *Merck*). H_2O_2 was standardized daily by manganometric analysis. Aq. stock solns. were prepared from doubly distilled, deionized H_2O. Solid I_2 (*Merck*; reagent grade, 99.8%) was stirred in doubly distilled H_2O for several hours. The soln. was filtered through *Pyrex* wool and stored in a glass-stoppered bottle protected from light. Antioxidants used: 2,5-DHBA (=2,5-dihydroxybenzoic acid; *Aldrich*; reagent grade, 98%), 2,6-DHBA (=2,6-dihydroxybenzoic acid; *Aldrich*; reagent grade, 98%), caffeic acid (= 3-(3,4-dihydroxyphenyl)prop-2-enoic acid; *Merck*; reagent grade, >98%), ferulic acid (= 3-(4-hydroxy-3-methoxyphenyl)prop-2-enoic acid; *Aldrich*; reagent grade, >99%), isoferulic acid (= 3-(3-hydroxy-4-methoxyphenyl)prop-2-enoic acid; *Merck*; reagent grade, >98%), hydroquinone (= benzene-1,4-diol; *Carlo Erba*; reagent grade, ≥99%), pyrocatechol (= benzene-1,2-diol; *Fluka*; reagent grade, ≥98%).

The kinetics of the subsystems (antioxidant $+ IO_3^- + H^+$) and (antioxidant $+ I_2 + H^+$) were followed spectrophotometrically by using a *Shimadzu UV-1601PC* spectrophotometer equipped with thermostatted cell compartments and magnetic microstirrer. The spectrophotometer was controlled by an *IBM*-compatible PC. The data acquisition program UVPC (*Shimadzu*) was used. The temp. was maintained constant at $25.0 \pm 0.1°$. Mixtures were prepared directly in a 1.000-cm optical path quartz cell by mixing of the appropriate amounts of stock solns. of reagents and using precision micropipettes. For the first subsystem, the order of addition was: H_2O, antioxidant, acidic iodate to a total volume of 3.0 ml. For the second subsystem, the order of addition was: $HClO_4$, antioxidant, and I_2 to a total volume of 3.0 ml. Recordings started immediately after the addition of the last reagent. Oscillations in the *BR* mixtures were followed potentiometrically by recording the potential of the soln. with a couple bright Pt-electrode (*Hamilton*, model *P/N 238945*)-reference electrode (double-junction Ag/AgCl electrode; *Ingold*, model *373-90-WTE-ISE-S7*). Electrodes were connected to a pH multimeter (*WTW*, model *pH 540 GLP*) controlled by an *IBM*-compatible PC. The accuracy of the multimeter was ±1 mV. The data-acquisition program Multi Achat II (*WTW*) was used. The multimeter was equipped with a temp. sensor with an accuracy of ± 0.1°.

BR Mixtures were prepared by mixing the appropriate amounts of stock solns. of reagents using pipets or burets in a 100-ml beaker to a total volume of 30 ml. The order of addition was: malonic acid, $MnSO_4$, $HClO_4$, $NaIO_3$, and H_2O_2. Oscillations started after the addition of H_2O_2. All solns. and reaction mixtures were maintained at constant temp. by means of a suitable thermostating system (accuracy $\pm 0.1°$). Inhibitory effects by antioxidants were studied by adding 1.0 ml of a suitable dil. soln. of antioxidant to 30 ml of an active *BR* mixture.

3. Results and Discussion. – 3.1. *Kinetics of Nonoscillating* BR *Subsystems + Inhibitor*. The reactions of acidic IO_3^- and of acidic I_2 with four different diphenolic antioxidants are outlined below. We study these because, in the complete oscillating system, these reactions must be occurring in parallel with HOO• radicals. The concentrations of antioxidants were one or two orders of magnitude greater in these experiments than those used to study the inhibitory effects on the *BR* reaction [1], to better follow the possible oxidation reactions of the inhibitors.

Subsystem IO_3^- (H^+) + 2,5-DHBA. In *Fig. 2,a*, the repeated spectra for this subsystem are reported. Spectra were repeated at intervals of 25 s for a total of 150 s in the wavelength range 500–250 nm. It can be noted that the characteristic peak of diphenols at *ca.* 310–330 nm drastically decreases with a simultaneous increase of a peak around 425 nm, at which wavelength quinones absorb. The reaction is fast because 2,5-DHBA is easily oxidized to the corresponding quinone by acidic IO_3^- (*Scheme 1*). *Fig. 2,b*, shows the behavior of absorbance at 329 nm *vs.* time. As can be seen, completion is reached in *ca.* 60 s. This confirms that the oxidation of 2,5-DHBA to the corresponding quinone is fast.

Scheme 1

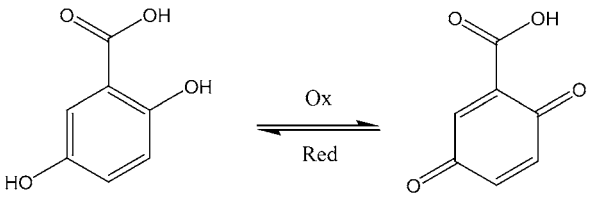

Subsystem IO_3^- (H^+) + 2,6-DHBA. In *Fig. 3,a*, the spectra for this subsystem, recorded again in the same 500–250 nm wavelength range at intervals of 4 min for a total of 30 min, show that, with this substrate, the oxidation reaction is very slow. *Fig. 3,b*, illustrates the behavior of absorbance at 308 nm *vs.* time. In this case, very little reaction takes place, and, after *ca.* 15 min, the rate becomes even slower. This is not surprising because *meta*-quinones are unknown, and it is difficult to hypothesize the formation of a semiquinone radical.

Subsystem IO_3^- (H^+) + Caffeic Acid (CA, sodium salt). In *Fig. 4,a*, the spectra for this system, repeated at intervals of 25 s to a total of 225 s in the wavelength range 500–250 nm, show a quick decrease of the peak at *ca.* 310 nm (diphenol peak) with a simultaneous increase near 400 nm that can be ascribed to the corresponding quinone peak. The reaction is quite fast because CA is easily oxidized to the corresponding quinone (*Scheme 2*). *Fig. 4,b* shows the behaviors of absorbances at *ca.* 310 nm and *ca.* 400 nm, establishing that the reaction is nearly complete after *ca.* 150 s.

Subsystem IO_3^- (H^+) + Ferulic Acid (FA, sodium salt). As can be seen from *Fig. 5,a* and *b*, this reaction is slower than that with CA. The spectra were recorded again at

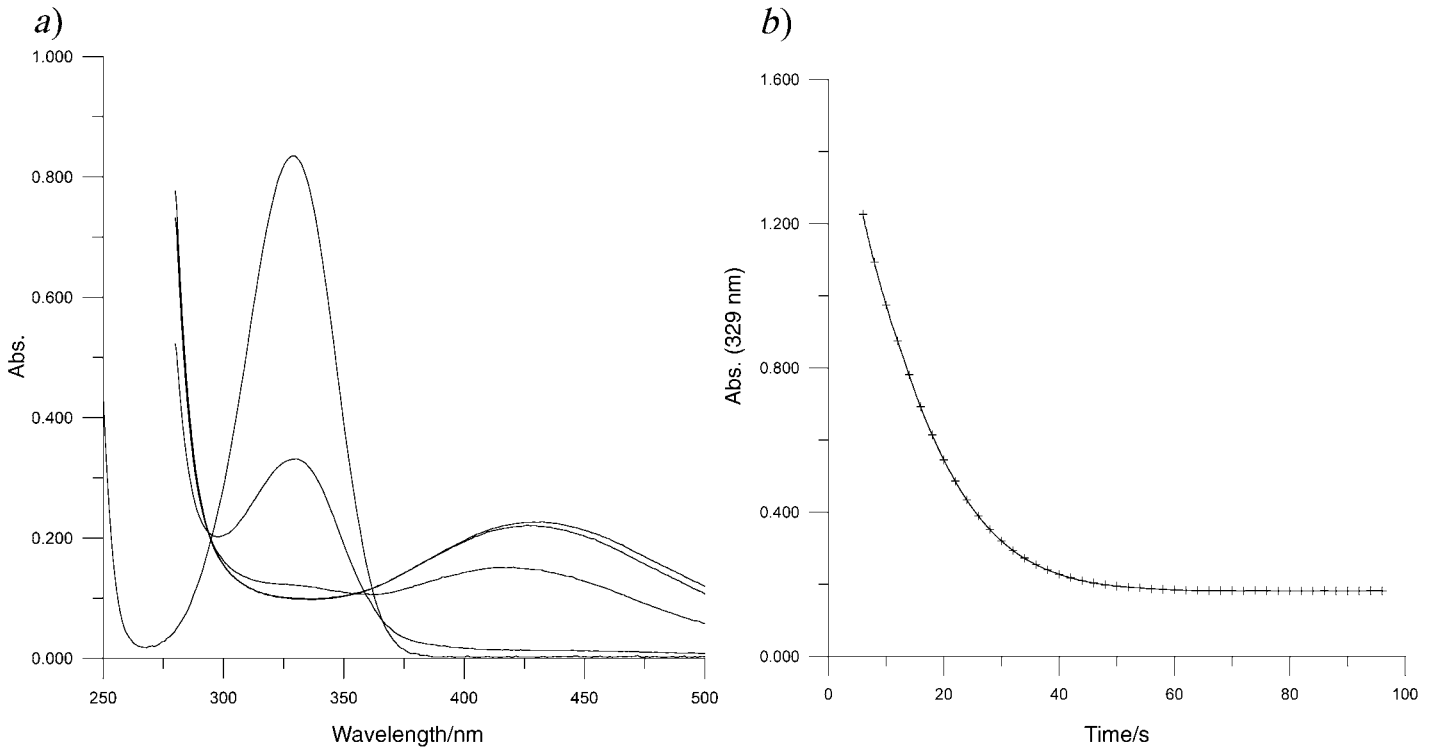

Fig. 2. a) *Repeated spectra of the subsystem* $IO_3^-(H^+)+2,5\text{-}DHBA$ (initial concentrations: $[IO_3^-]=3.33\cdot10^{-2}$ M, $[HClO_4]=2.66\cdot10^{-2}$ M, $[2,5\text{-DHBA}]=2.16\cdot10^{-4}$ M). b) *Behavior of absorbance at 329 nm* vs. *time.*

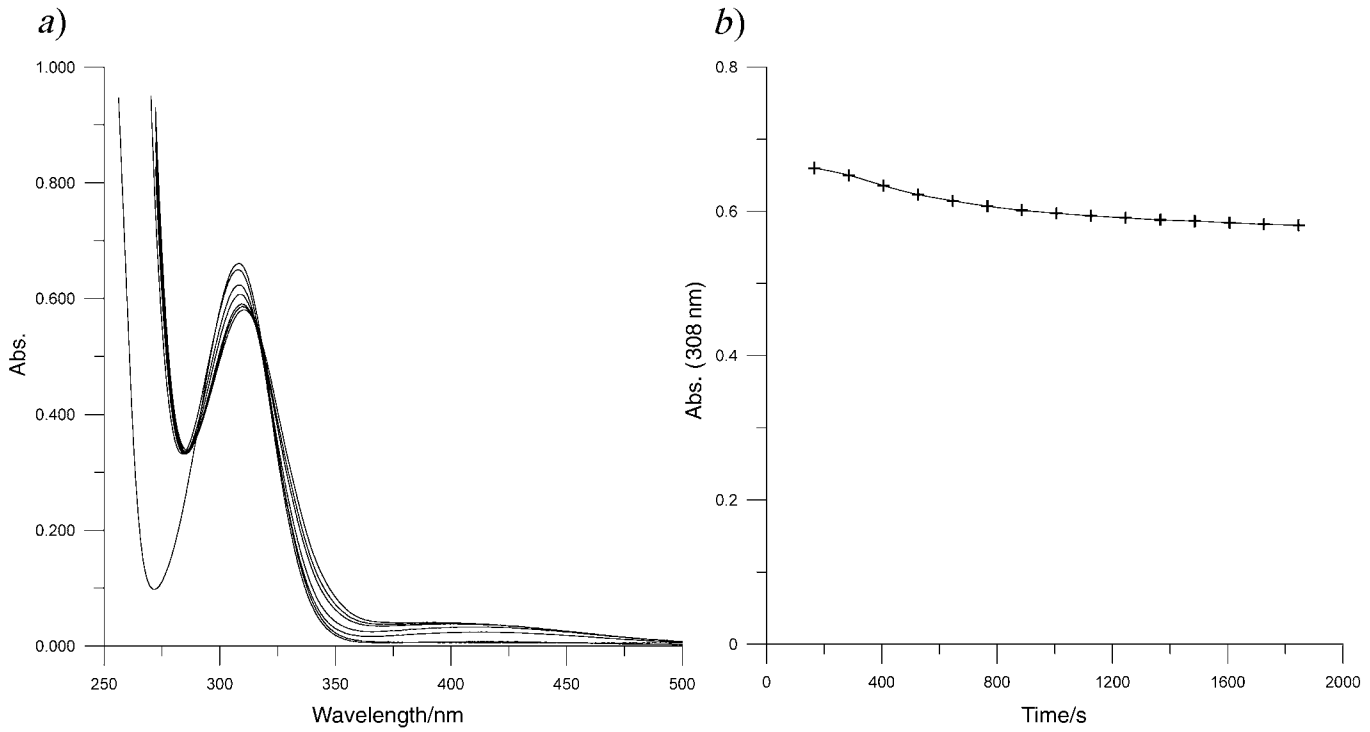

Fig. 3. a) *Repeated spectra of the subsystem* $IO_3^-(H^+) + 2,6\text{-}DHBA$ (initial concentrations: $[IO_3^-] = 3.33 \cdot 10^{-2}$ м, $[HClO_4] = 2.66 \cdot 10^{-2}$ м, $[2,6\text{-DHBA}] = 2.16 \cdot 10^{-4}$ м). b) *Behavior of absorbance at 308 nm* vs. *time.*

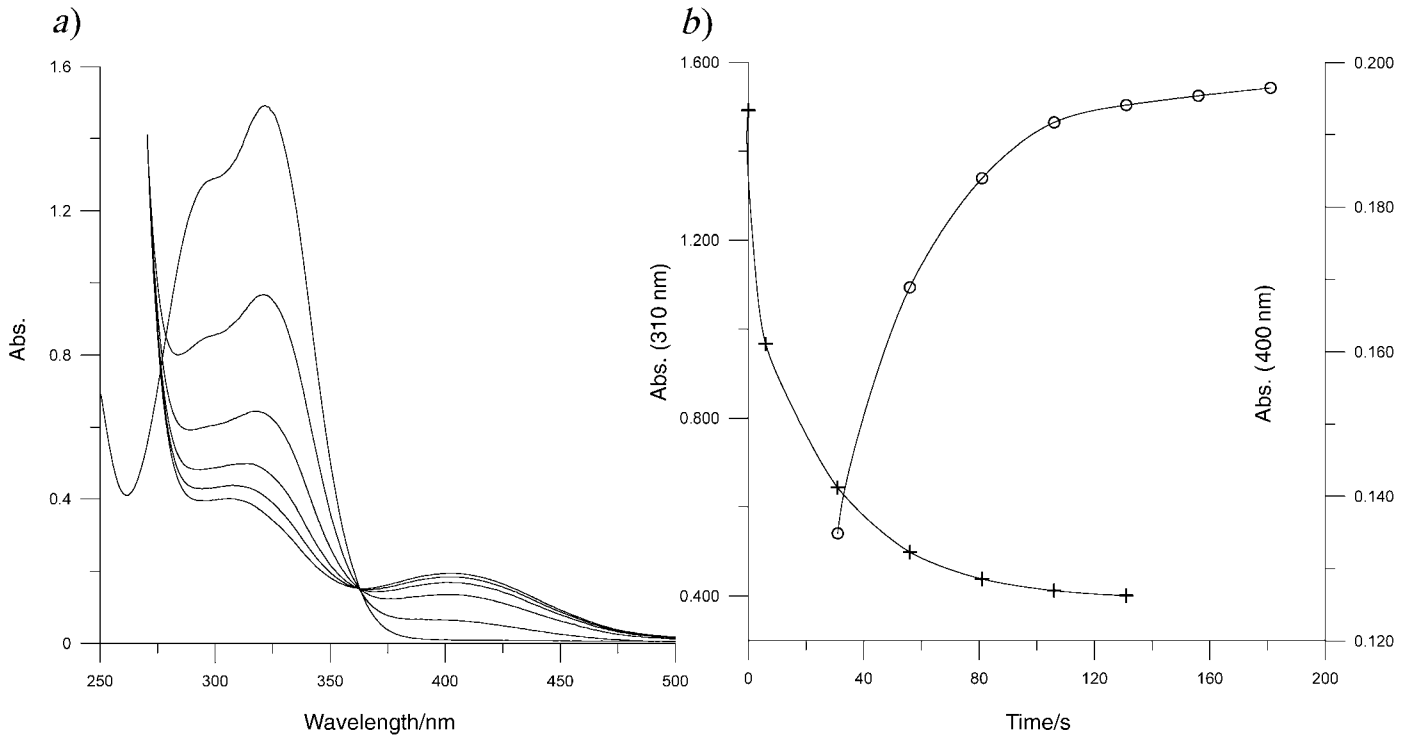

Fig. 4. a) *Repeated spectra of the subsystem* $IO_3^-(H^+)$ + *caffeic acid sodium salt* (initial concentrations: $[IO_3^-] = 3.33 \cdot 10^{-2}$ M, $[HClO_4] = 2.66 \cdot 10^{-2}$ M, $[CA] = 1.85 \cdot 10^{-4}$ M). b) *Behaviors of absorbances at 310 and 400 nm* vs. *time.*

Scheme 2

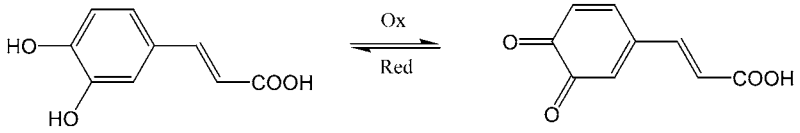

intervals of 2 min to a total of 26 min. The reaction is nearly complete after *ca.* 26 min. The slowness of oxidation of FA is probably due to the MeO group, which would be much slower to oxidize than the comparable OH group of CA.

In both IO_3^- (H^+) + DHBA subsystems the absence of isosbestic points in the repeated spectra could imply the occurrence of another reaction besides the oxidation: a possibility could be some ring iodination. By contrast, the reactions of CA and FA give rise to a well-defined isosbestic point at 362 nm, which allows us to conclude that a well-defined oxidation product is formed. The experimental results with IO_3^- (H^+) establish that 2,5-DHBA, CA, FA, and 2,6-DHBA are all oxidized to quinones by acidic IO_3^- at rates differing by more than two orders of magnitude, fastest to slowest in the order listed.

Next, reactions of acidic I_2 with the same four antioxidants were studied. I_2 is produced periodically in the complete *BR* oscillator. It is consumed there by malonic acid. Whenever I_2 is present, HOI is also present from hydrolysis, and either or both are able to iodinate and/or oxidize diphenols.

Subsystem I_2 (H^+) + 2,5-DHBA. I_2 (in equilibrium with I(I)) can either oxidize diphenols (being reduced to I^-) or substitute for H(s) in the aromatic ring. In *Fig. 6,a*), the repeated spectra for the system $I_2(H^+)$ + 2,5-DHBA are reported in the wavelength range 500 – 250 nm. The bold traces refer to solutions of 2,5-DHBA alone and I_2 alone at the same concentrations as those in the initial reaction mixture. Repeated spectra (regular traces) were recorded at intervals of 80 s for a total of 800 s. The I_3^- species has peaks near 280 and 353 nm and initially increases (as I^- forms), then decreases (as I_2 decreases). The peak at *ca.* 290 nm is due mostly to I_3^-, the peak at 328 nm is a composite of I_3^- and 2,5-DHBA. The peak at 460 nm is a composite of the decreasing I_2 and the increasing quinone. This interpretation is supported by the behaviors of the absorbances at 290, 328.6, and 460 nm *vs.* time reported in *Fig. 6,b*. Reaction is nearly complete after *ca.* 18 min. It is well known that phenol reacts in solution with I_2 to form a triiodo product. Presumably, substitution or multi-substitution is a possibility with diphenols such as 2,5-DHBA. There is also the possibility that substituted diphenols are oxidized to the corresponding quinones. This is too complex to sort out from UV/VIS spectra.

Subsystem I_2 (H^+) + 2,6-DHBA. Repeated spectra, shown in *Fig. 7,a*, were recorded as described for the previous system. The bold trace refers to a solution of 2,6-DHBA alone at the same concentration as in the initial reacting mixture. In this case, we can observe a noticeable initial increase of a peak around 318 nm, shifted by *ca.* 10 nm from the peak of 2,6-DHBA. The peak at 318 nm is broader than that of 2,6-DHBA. This peak decreases with time. Since 2,6-DHBA forms, not a quinone, but, at most, a semiquinone radical as previously stated, we think that the main reaction is the iodination of the ring. In fact, positions 3 and 5 are highly favored. The peak of I_2 at

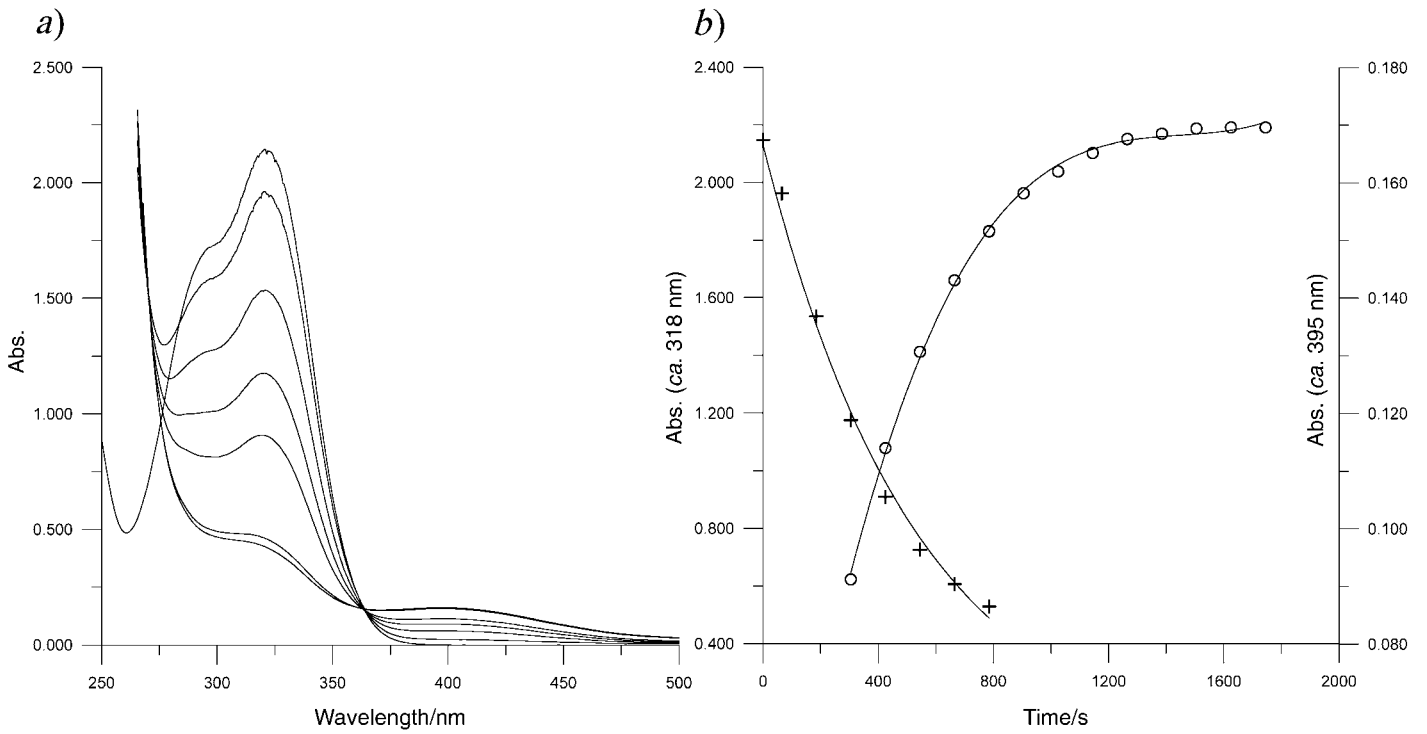

Fig. 5. a) *Repeated spectra of the subsystem* $IO_3^-(H^+)$ + *ferulic acid sodium salt* (initial concentrations: $[IO_3^-] = 3.33 \cdot 10^{-2}$ M, $[HClO_4] = 2.66 \cdot 10^{-2}$ M, $[FA] = 1.72 \cdot 10^{-4}$ M). b) *Behaviors of absorbances at 318 and at 395 nm* vs. *time.*

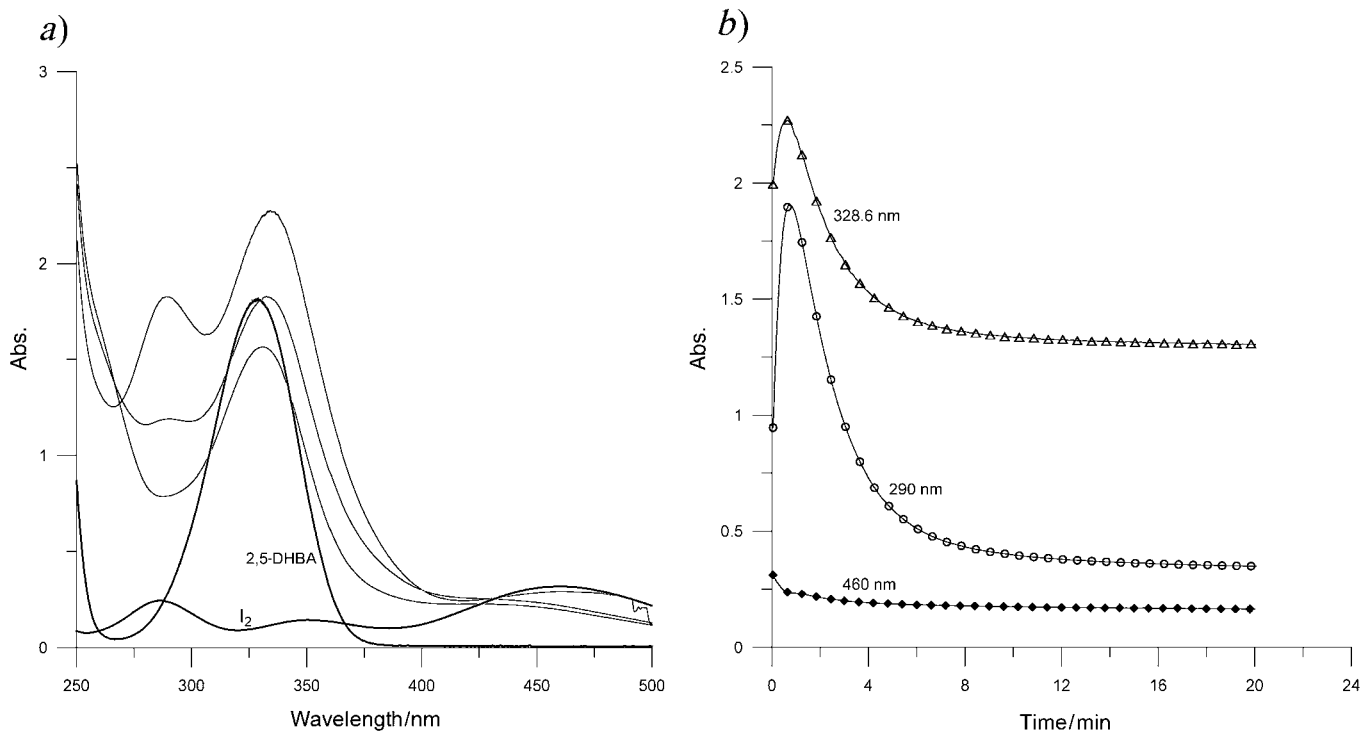

Fig. 6. a) *Repeated spectra of the subsystem* $I_2(H^+) + 2,5\text{-}DHBA$ (initial concentrations: $[I_2] = 2.41 \cdot 10^{-4}$ м, $[HClO_4] = 2.66 \cdot 10^{-2}$ м, $[2,5\text{-DHBA}] = 2.16 \cdot 10^{-4}$ м). b) *Behaviors of absorbances at 328.6, 290, and 460 nm* vs. *time.*

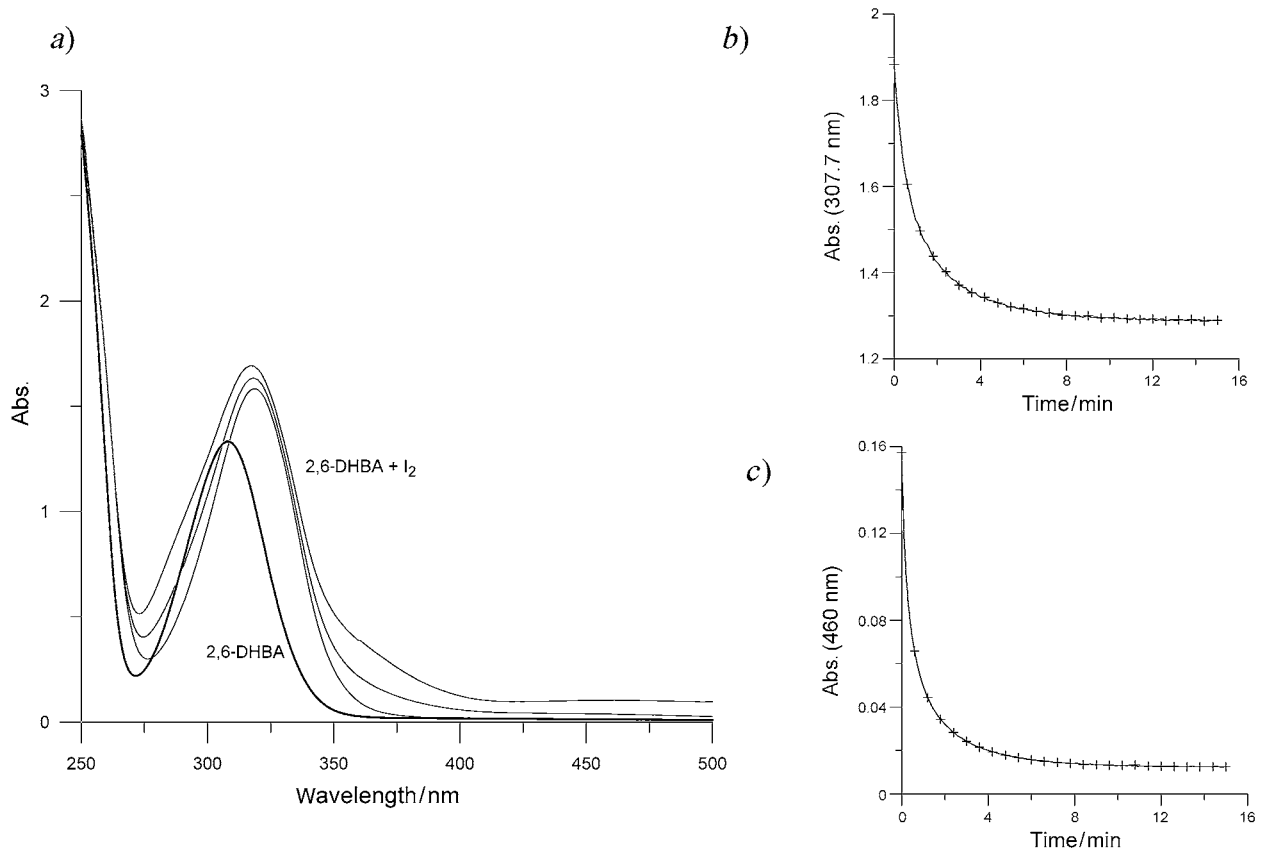

Fig. 7. a) *Repeated spectra of the subsystem* $I_2(H^+) + 2,6\text{-}DHBA$ (initial concentrations: $[I_2] = 2.41 \cdot 10^{-4}$ M, $[HClO_4] = 2.66 \cdot 10^{-2}$ M, $[2,6\text{-DHBA}] = 2.16 \cdot 10^{-4}$ M). b) *Behavior of absorbance at 307.7 nm* vs. *time*. c) *Behaviour of absorbance at 460 nm* vs. *time*.

460 nm decreases with time. The behaviors of absorbances at *ca*. 308 and 460 nm *vs.* time are shown in *Fig. 7*, *b* and *c*, respectively.

Subsystem I_2 (H^+) + Caffeic Acid (CA, sodium salt). As above, the bold trace shown in *Fig. 8*, *a*, refers to a solution of CA alone at the same concentration as in the initial reacting mixture. Repeated spectra were recorded at 86 s intervals for a total of 860 s plus three other spectra after 5, 30, and 60 min, respectively. The peak at 321 nm, characteristic of CA, decreases with time, as does the peak of I_2 at 460 nm. Since CA is able to form the corresponding quinone as stated previously, we think that both oxidation and iodination can occur. In *Fig. 8*, *b* and *c*, respectively, the behaviors of absorbances at 321 and 460 nm *vs.* time are reported.

Subsystem I_2 (H^+) + Ferulic Acid (FA, sodium salt). Repeated spectra of the reacting mixture were recorded at 80-s intervals for a total of 800 s plus another spectrum after 10 min (*Fig. 9*, *a*). One can note the decrease with time of the peak at *ca*. 321 nm, characteristic of FA, and the simultaneous decrease of the I_2 peak at 460 nm. As previously stated, the MeO group would be much slower to oxidize than the comparable OH group of CA. Thus, iodination is presumably the main reaction in this subsystem. Near 370 nm, there is a region with little change. We are inclined to think the reaction is not complete enough to cause much change, but it looks like at *ca*. 400 nm, the decrease due to I_2 might be balanced by an increase due to quinone. Thus it could be some oxidation plus the iodination. In *Fig. 9*, *b* and *c*, respectively, the behaviors of absorbances at 321 and 460 nm *vs.* time are reported.

Except for the 2,6-DHBA, the reactions of inhibitors with I_2 in acidic medium are much slower than the reactions with acidic IO_3^-, where the half-life for antioxidants + acidic IO_3^- are of the order of 20 – 200 s. The half-lives with I_2 are from 2 to 20 times longer.

A scheme of the possible reactions of an inhibitor of the generic $Ar(OH)_2$ form in the complete *BR* oscillator is reported in *Scheme 3*. Therein, ArO_2 and $Ar(OH)O^{\bullet}$ represent the corresponding quinone or semiquinone radical respectively. Rate constants for the various steps (not necessarily elementary) will be discussed in the next section.

3.2. *Mechanistic Interpretation.* 3.2.1. *Simulations for the Completely Inhibited* BR *Oscillator.* We have previously described a method for using inhibition times in the *BR* reaction as a measure of antioxidant activity and have shown how we used data for caffeic acid to arrive at values for k_{IN} and k_{DEG} [1]. We now used data from this previous study to calculate values for k_{IN} and k_{DEG} for a series of antioxidants. The constants are those for the *Eqns. 1* and *2* shown in *Sect. 1:* an inhibition step, *IN*, in which the radical $HOO^{\bullet}$ is reduced by the phenol, and a degradation step, *DEG*, in which the antioxidant is converted to other products. While we believe those steps are important and help us to understand the general inhibition process, they are essentially empirical. That is, the actual processes are much more complex. We shall speak of complexities later in this section.

Inhibition data from [1] were used for two runs for each of the antioxidants, each run being performed at a different concentration of antioxidant. A trial and error process was used with the *Gepasi* simulator [9] to find the unique set of k_{IN} and k_{DEG} that best simulated the inhibition time for both concentrations. Those constants are shown in *Table 2*. Inhibitory effects by hydroquinone (= benzene-1,4-diol) were studied in this work following the procedure outlined in *Sect. 2* (*Experimental*).

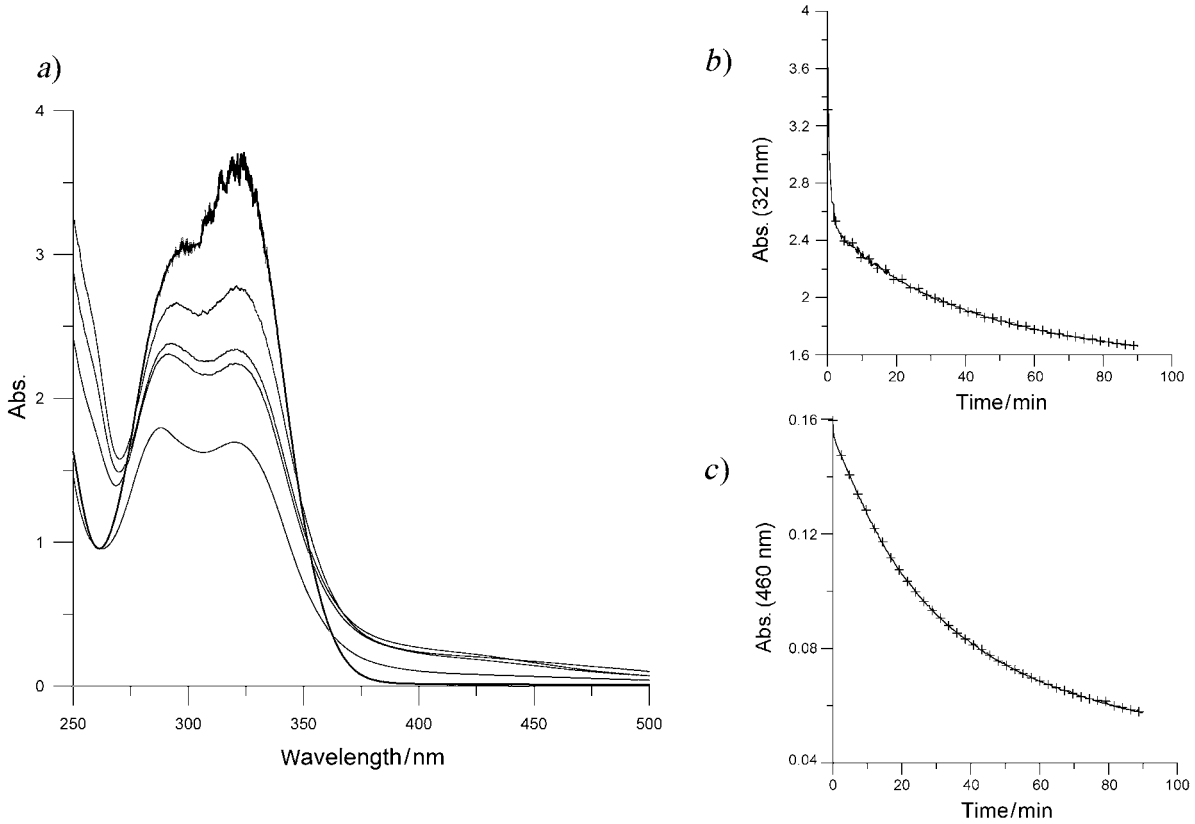

Fig. 8. a) *Repeated spectra of the subsystem* $I_2(H^+)$ + *caffeic acid sodium salt* (initial concentrations: $[I_2] = 2.41 \cdot 10^{-4}$ M, $[HClO_4] = 2.66 \cdot 10^{-2}$ M, $[CA] = 1.85 \cdot 10^{-4}$ M). b) *Behavior of absorbance at 321 nm* vs. *time.* c) *Behaviour of absorbance at 460 nm* vs. *time.*

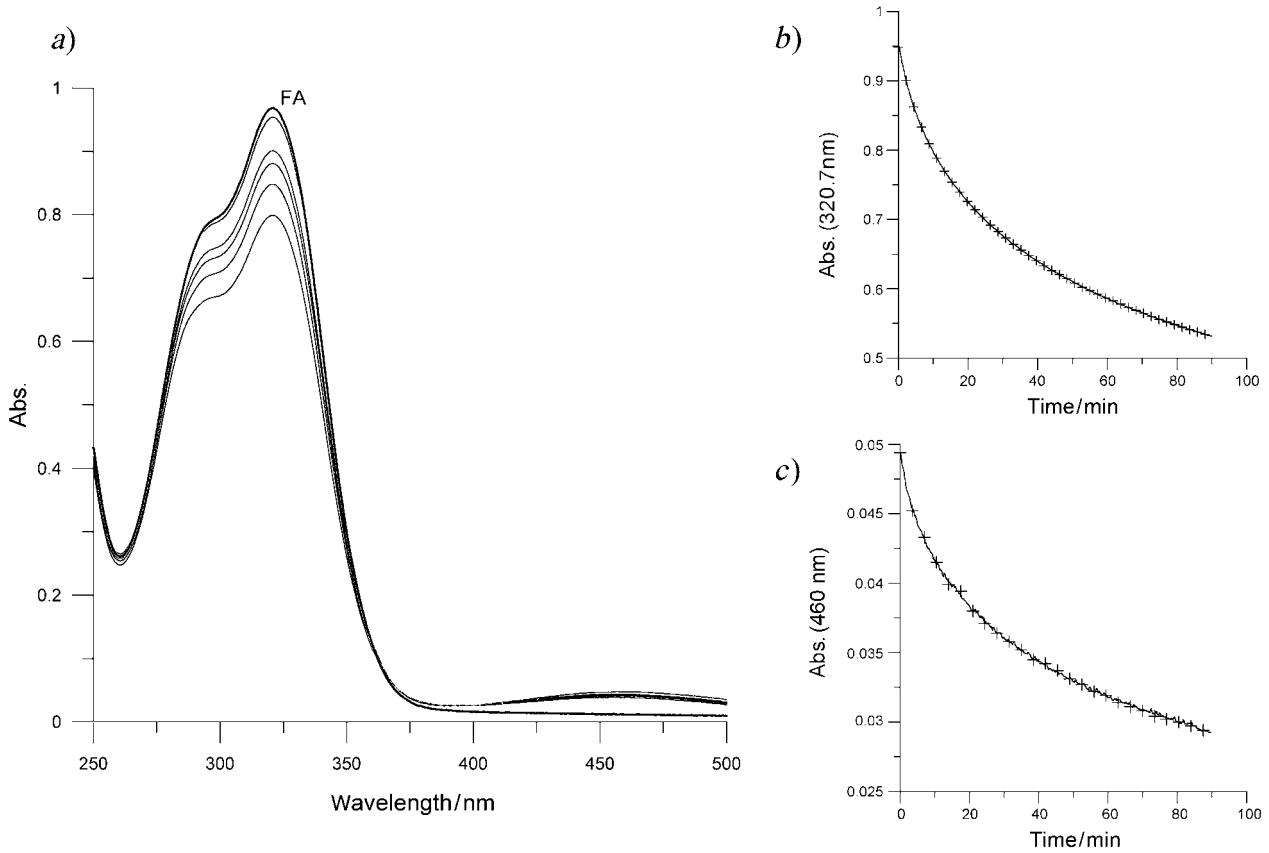

Fig. 9. a) *Repeated spectra of the subsystem $I_2(H^+)$ + ferulic acid sodium salt* (initial concentrations: $[I_2] = 2.41 \cdot 10^{-4}$ M, $[HClO_4] = 2.66 \cdot 10^{-2}$ M, $[FA] = 1.72 \cdot 10^{-4}$ M). b) *Behavior of absorbance at 302.7 nm* vs. *time*. c) *Behaviour of absorbance at 460 nm* vs. *time*.

Scheme 3. *Possible Reactions of an Inhibitor of the Generic Ar(OH)$_2$ Form in a Complete* BR *Oscillator*

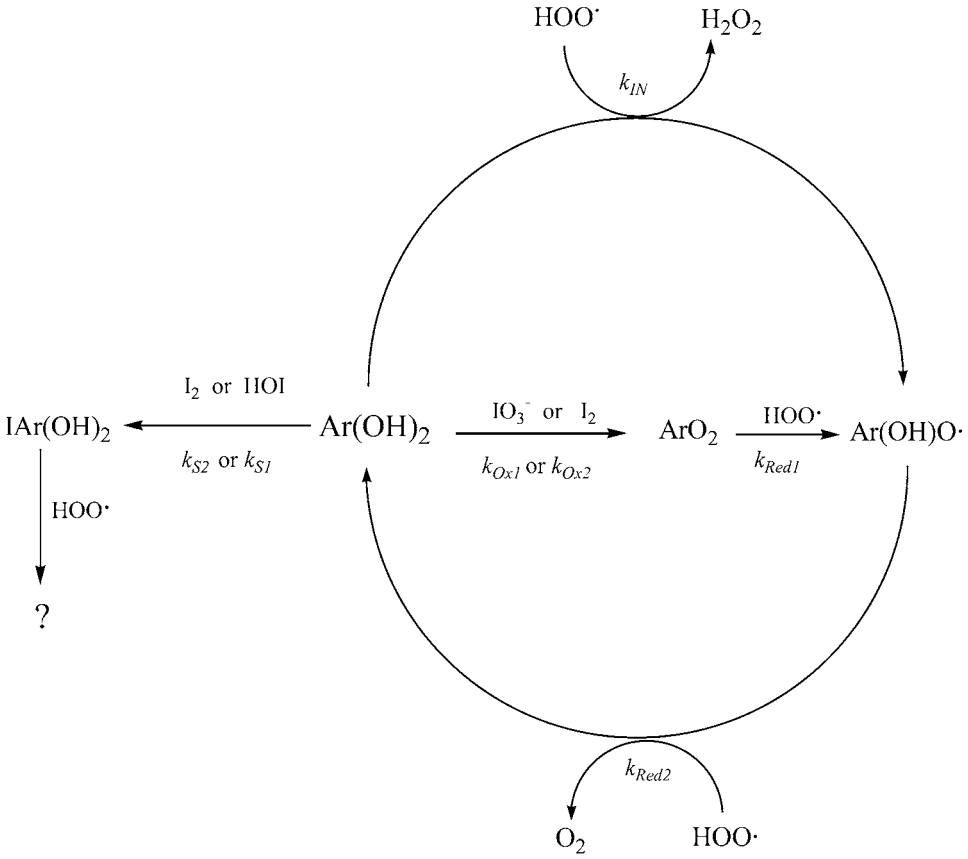

Table 2. *Calculated Rate Constants* k_{IN} *and* k_{DEG} *from Inhibition Data Reported in* [1][a])

	k_{IN} [M^{-1} s^{-1}]	k_{DEG} [s^{-1}]
2,4-DHBA	$7.6 \cdot 10^6$	$2.0 \cdot 10^{-4}$
2,5-DHBA	$2.4 \cdot 10^5$	0
2,6-DHBA	$5.6 \cdot 10^7$	$1.2 \cdot 10^{-3}$
3,4-DHBA	$2.2 \cdot 10^7$	$7.0 \cdot 10^{-4}$
3,5-DHBA	$7.2 \cdot 10^6$	$2.5 \cdot 10^{-4}$
Re	$1.2 \cdot 10^7$	$3.0 \cdot 10^{-4}$
PC	$2.0 \cdot 10^7$	0
CA	$8.0 \cdot 10^7$	$6.4 \cdot 10^{-4}$
FA	$8.9 \cdot 10^7$	$6.6 \cdot 10^{-4}$
HA	$1.3 \cdot 10^8$	$1.0 \cdot 10^{-3}$

[a]) DHBA = Dihydroxybenzoic acid; Re = resorcinol = benzene-1,3-diol; PC = pyrocatechol = benzene-1,2-diol; CA = caffeic acid = 3-(3,4-dihydroxyphenyl)prop-2-enoic acid; FA = ferulic acid = 3-(4-hydroxy-3-methoxyphenyl)prop-2-enoic acid; HA = homovanillic acid = 4-hydroxy-3-methoxybenzoic acid.

By using only the values of k_{IN}, the relative activities (*r.a.*) of the antioxidants compared to resorcinol as a standard ($r.a. = k_{IN}(\text{diphenol})/k_{IN}(\text{Re})$) fall in the order HA (10.8) > FA (7.4) > CA (6.7) > 2,6-DHBA (4.7) > 3,4-DHBA (1.8) ~ PC (1.7) > Re (1.0; standard) > 2,4-DHBA (0.63) ~ 3,5-DHBA (0.60) > 2,5-DHBA (0.023). The activities for these compounds based on relative activity with respect to inhibition times (*r.a.t.*) are [1] PC (5.73) > FA (2.27) ≥ CA (2.21) > 2,6-DHBA (1.74) ≥ HA (1.65) > 3,4-DHBA (1.27) > Re (1.00; standard) > 2,4-DHBA (0.50) ≥ 3,5-DHBA (0.40) > 2,5-DHBA (*ca.* 0.0).

Except for homovanillic acid (HA) and pyrocatechol (PC), the order of activities is the same for both methods. It is not unexpected that the order for relative values of k_{IN} shows some correlation with the activity based on experimental inhibition times, since k_{IN} is more important in the simulations than k_{DEG}, although, of course, both play a role. Realizing that both processes *IN* and *DEG* are oversimplified composite processes, we attempted in the following to look at some of the processes that could lead to degradation of the antioxidant.

3.2.2. *Simulations for the Nonoscillating Subsystems + Inhibitor. Oxidation of Diphenols by IO_3^- (H^+).* The reaction of *ortho*- or *para*-diphenols with acidic IO_3^- to form I_2 and quinones must involve the steps (not necessarily elementary of *Eqns. 3–6*). The step of *Eqn. 3* was assumed to be rate-determining. *ortho*-Quinones are known to be unstable in aqueous solution; however, the half-life of 1,2-quinone under conditions of our experiments is over 1 h as measured by absorbance in the near 400 nm. Since I_2 forms rapidly, HOIO must be reduced rapidly according to *Eqn. 4*. Likewise, HOI must be reduced rapidly according to *Eqn. 5*. Rate constants for the two reactions of *Eqns. 4* and *5* were arbitrarily chosen to be large enough so as to be non-rate-determining. As soon as some I^- is formed, iodine equilibria and reactions between oxyiodine species (reactions *I1*, *I2*, and *I3*) can take place. The net result with excess IO_3^- is given by *Eqn. 6*.

$$Ox1\ \ H^+ + IO_3^- + Ar(OH)_2 \rightarrow HOIO + ArO_2 + H_2O \tag{3}$$

$$HOIO + Ar(OH)_2 \rightarrow HOI + ArO_2 + H_2O \tag{4}$$

$$HOI + Ar(OH)_2 \rightarrow H^+ + I^- + ArO_2 + H_2O \tag{5}$$

$$5\ Ar(OH)_2 + 2\ H^+ + 2\,IO_3^- \rightarrow 5\ ArO_2 + I_2 + 6\ H_2O \tag{6}$$

meta-Quinones are unknown, and oxidation of *meta*-diphenols is very slow. The products have not been identified, but a product peak near 400 nm indicates some quinone formation, possibly an *ortho*- or *para*-hydroxyquinone, coming from an initial oxidation to a benzenetriol (1,2,3- or 1,3,4-).

Oxidation of Diphenols by I_2. I_2 can react with diphenols without IO_3^- present. *ortho*- and *para*-Diphenols can be oxidized to quinones according to *Eqn. 7*. The triiodide equilibrium of *Eqn. 8* becomes significant. Triiodide-ion concentration first increases as $[I^-]$ increases, and then decreases as $[I_2]$ is consumed. The time of the maximum in $[I_3^-]$ is related to the rate constant for oxidation. It is possible that the true oxidizing agent in the process *Ox2* is HOI. However, the reaction with HOI would require that the rate constant be near or greater than diffusion-controlled, so a direct reaction with I_2 was assumed for simulation purposes.

$$Ox2\ \mathrm{Ar(OH)_2} + \mathrm{I_2} \rightarrow \mathrm{ArO_2} + 2\,\mathrm{H^+} + 2\,\mathrm{I^-} \tag{7}$$

$$\mathrm{I_2} + \mathrm{I^-} \rightleftarrows \mathrm{I_3^-} \tag{8}$$

Iodine Substitution. Another possibility for reaction is iodination of the aromatic ring by electrophilic substitution. Iodination may be accomplished by HOI or by I_2. Di- or trisubstitution can occur, and the iodinated compounds could still be oxidized to quinones, at different rates, resulting in the overall reaction of *Eqn. 11* where Ar′ has *n* fewer H atoms than Ar.

$$n\ \mathrm{I_2} + n\ \mathrm{H_2O} \rightleftarrows n\ \mathrm{H^+} + n\ \mathrm{I^-} + n\ \mathrm{HOI} \tag{9}$$

$$S1\ \mathrm{Ar(OH)_2} + n\ \mathrm{HOI} \rightarrow \mathrm{Ar'(OH)_2I}_n + n\ \mathrm{H_2O} \tag{10}$$

$$S2\ n\ \mathrm{I_2} + \mathrm{Ar(OH)_2} \rightarrow \mathrm{Ar'(OH)_2I}_n + n\ \mathrm{H^+} + n\ \mathrm{I^-} \tag{11}$$

When IO_3^- is present, I^- is reoxidized to I_2 by the *Dushman* reaction (*Eqn. 12*). Reactions with HOI will become less important in solutions without IO_3^- because [I^-] build-up will cause [HOI] to decrease. Indeed, oxidation of pyrocatechol and resorcinol both take place in solution with I_2 and excess I^-. In these solutions, [HOI] is very low. HOI can undergo addition to unsaturated side chains in CA and FA. Addition to a side-chain C=C bond is expected to be slower than substitution in the ring, but could be an additional sink for I_2. If I_2 iodine is incorporated into the ring or into the side chain, the stoichiometry differs from that of oxidation alone (*Eqn. 13*). Presumably the iodinated diphenol can still be oxidized to an iodinated quinone but quinones are not readily substituted by HOI.

$$6\ \mathrm{H^+} + 5\ \mathrm{I^-} + \mathrm{IO_3^-} \rightarrow 3\ \mathrm{I_2} + 3\ \mathrm{H_2O} \tag{12}$$

$$(2n+1)\ \mathrm{Ar(OH)_2} + n\ \mathrm{H^+} + n\ \mathrm{IO_3^-} \rightarrow 2n\ \mathrm{ArO_2} + \mathrm{Ar'(OH)_2I}_n + 3n\ \mathrm{H_2O} \tag{13}$$

For the iodination of the diphenols described here, the substitution and/or addition reactions with I_2 or HOI are relatively slow compared with oxidation reactions. Although iodination is certainly occurring in the systems studied here, we believe the predominant reactions involve oxidation, and those are the ones we focus on in the following section.

Reactions of Antioxidants in the Oscillating System. In the oscillating reactions where inhibition takes place, [IO_3^-] is orders of magnitude greater than [I_2], so the oxidation of diphenols to quinones by iodate is much more important than the reactions with I_2. For the *ortho*- and *para*-diphenolic antioxidants used in this work in the *BR* reaction, the conversion to quinones would be espected to be complete long before the inhibition period ends. Thus the *DEG* step is not simply oxidation to quinone. The quinones must also have antioxidant properties.

A summary of 'rate constants' for oxidation by IO_3^- and by I_2 is given in *Table 3*. They are not the result of rigorous kinetic studies but rather values determined from the *Gepasi* simulator to give reasonable approximations to the experimental curves from spectrophotometric data. The reactions assumed are those listed above in this section, *e.g.*, with I_2 present, reaction *Ox2* (*Eqn. 7*) was assumed to be rate determining,

Table 3. *Approximate Rate Constants for Oxidation of Some Diphenols Ar(OH)$_2$ by Iodate and Diiodine*

Diphenol	k for IO_3^- [a]) [M^{-2} s^{-1}]	k for I_2 [b]) [M^{-1} s^{-1}]	[Diphenol] [μM]	Time for 90% oxidation [c]) [s]	Inhibition time [d]) [s]
CA	8	1.5	7	102	2501
FA	1	1.2	6	500	2265
PC	50	50	7	26	5624
2,5-DHBA	30	40	108	18	1341
Hydroquinone	120	10	45	12	83

[a]) k_{Ox1}. [b]) k_{Ox2}; initial conditions: $[I_2] = 4.43 \cdot 10^{-4}$ M, $[HClO_4] = 0.0266$M. [c]) Oxidation by IO_3^-. [d]) Inhibition in oscillator; initial conditions: $[H_2O_2] = 1.20$M, $[HClO_4] = 0.0266$M, $[IO_3^-] = 0.0667$M, [malonic acid] = 0.050M, $[Mn^{2+}] = 0.00667$M.

and the rate law was assumed to have the form: $-\mathrm{d}[\mathrm{Ar(OH)_2}]/\mathrm{d}t = k_{Ox2}[\mathrm{I_2}][\mathrm{Ar(OH)_2}]$. The value of k_{Ox2} was chosen to give the best agreement with spectrophotometric data of the type shown in *Figs. 7–9*. Once an approximate k_{Ox2} was known, it was incorporated into the simulation, and k_{Ox1} was determined from data with IO_3^- present (*cf. Eqn. 3*), assuming the rate law $-\mathrm{d}[\mathrm{Ar(OH)_2}]/\mathrm{d}t = k_{Ox1}[\mathrm{H^+}][\mathrm{IO_3^-}][\mathrm{Ar(OH)_2}]$. The goal was to find 'order-of-magnitude' constants to see whether reaction with IO_3^- or I_2 was important in degradation of the diphenols. I_2 Concentration is roughly two orders of magnitude lower than IO_3^- concentration in these oscillators, so most of the oxidation would be done by IO_3^-.

Oxidation of *ortho*- and *para*-diphenols to quinones, expecially by IO_3^-, is indeed rather fast compared to inhibition times. We conclude that the values for k_{IN} are composite values for processes that consume HOO$^\bullet$ radicals by both phenols and quinones, and likewise, k_{DEG} is a composite depending on degradation of both phenols and quinones to nonactive oxidation or iodinated products.

Since oxidation times are fast compared with inhibition times, we propose that quinones must also react readily with HOO$^\bullet$ radicals. In the *BR* mixtures, the reduction of the quinones back to diphenols by HOO$^\bullet$ radicals is thermodynamically possible. The standard reduction potential of HOO$^\bullet$ radicals to H_2O_2 is $+1.44$ V, the standard reduction potential of O_2 to HOO$^\bullet$ radicals is -0.046 V [10]. Thus HOO$^\bullet$ radicals have the potentials to be rather strong oxidizing and reducing agents, so we propose the reactions of *Eqns. 14* and *15*. These two steps together could maintain a small reservoir of diphenol while both quinone and diphenol deplete HOO$^\bullet$ radicals. The quinones, meanwhile, undergo degradation to form unknown products, which themselves may react further with either HOI or HOO$^\bullet$ radicals.

$$\textit{Red1}\ \mathrm{ArO_2} + \mathrm{HOO^\bullet} \rightarrow \mathrm{Ar(OH)O^\bullet} + \mathrm{O_2} \tag{14}$$

$$\textit{Red2}\ \mathrm{Ar(OH)O^\bullet} + \mathrm{HOO^\bullet} \rightarrow \mathrm{Ar(OH)_2} + \mathrm{O_2} \tag{15}$$

Furthermore, the radicals in the system may couple or cross-couple to form still other products of unknown composition and reactivity. In short, we know too little about the products to effectively model the system much beyond the empirical *IN* and *DEG* steps previously mentioned (*Eqns. 1* and *2*). With *meta*-diphenols, those two

steps may account for most of the observed inhibitions; with *ortho*- and *para*-diphenols, quinones must play a very important role.

3.3. *Effect of Temperature.* In the previous work [1], it was observed that the temperature of active uninhibited and inhibited *BR* mixtures rises slightly in spite of the thermostasis. For this reason, the temperature of the reacting mixtures was monitored during all the reactions with a temperature sensor, then an average temperature was calculated. With regard to the noninhibited *BR* reaction, some studies have shown that the inverse of the oscillatory time ($1/d$) *vs.* the temperature T shows an *Arrhenius* behavior [11][12]. This result was verified in the present work by using an uninhibited aqueous *BR* mixture that gave a long duration of oscillations, in order to study the dependence of this parameter on the temperature. The mixture had the following initial composition: [malonic acid] = 0.05M, $[Mn^{2+}] = 0.00667$M, $[HClO_4] = 0.0266$M, $[IO_3^-] = 0.0333$M, and $[H_2O_2] = 1.2$M. The study was made in the temperature range 295 K $\leq T \leq$ 213 K. The results are presented in *Table 4*. The inverse of the oscillatory time $1/d$ as a function of the temperature T is reported in *Fig. 10,a*) and clearly exhibits *Arrhenius* behavior. Plots of the logarithm of rate constants *vs.* $1/T$ are frequently used to obtain values of the activation energy but in the case of a *BR* reaction, there is no reason to expect the temperature coefficient to be related to a well-established activation energy. However, a plot of $\log(1/d)$ against $(1/T)$ yields a straight line (see *Fig. 10,b*), $R^2 = 0.9986$) from whose slope an approximate apparent 'average activation energy' (E_{av}) value of 68 ± 2 kJ for the overall oscillatory regime is found. This 'average activation energy' is to be compared to that obtained by *Ramaswami* and *Ganapathisubramanian* (57.3 kJ) [13]. The difference between these two values is due to the dependence of the apparent 'average activation energy' on the initial concentrations of the reagents in the mixture. *Ramaswami* and *Ganapathisubramanian* have used the following initial composition: [malonic acid] = 0.05M, $[Mn^{2+}] = 0.006$M, $[H_2SO_4] = 0.025$M, $[IO_3^-] = 0.06$M, and $[H_2O_2] = 1.2$M.

We have further investigated the dependence of inhibition times (t_i) and the time length of the resumed oscillations (d_r) on the temperature for four antioxidants (ferulic acid, isoferulic acid, caffeic acid, and 2,5-DHBA). Plots of $1/t_i$ and $1/d_r$ (in s^{-1}) *vs.* T show *Arrhenius* behaviors. Also in these cases, apparent 'average activation energies' can be calculated from the straight lines of $\log(1/t_i)$ *vs.* $1/T$ (E_{ti}) and from the straight lines $\log(1/d_r)$ *vs.* $1/T$ (E_{dr}). The results are reported in *Table 5*. Quoted errors were calculated by the procedure suggested by *Harris* [13]. A comparison between the apparent 'average activation energy' of the uninhibited reaction ($E_{av} = 68 \pm 2$ kJ) with the values of E_{t_i} and E_{d_r} reported in *Table 5*, taking also into account the experimental

Table 4. *Temperature and Duration of Oscillations for the Noninhibited* BR *Mixture*

Temp. of the thermostatic bath [°]	Average temp. of the reaction mixture [°]	Average temp. of the reaction mixture [K]	Oscillatory time d [s]
22	22.39	295.54	975
25	25.19	298.34	775
30	29.47	302.62	524
35	33.71	306.86	370
40	38.10	311.25	242

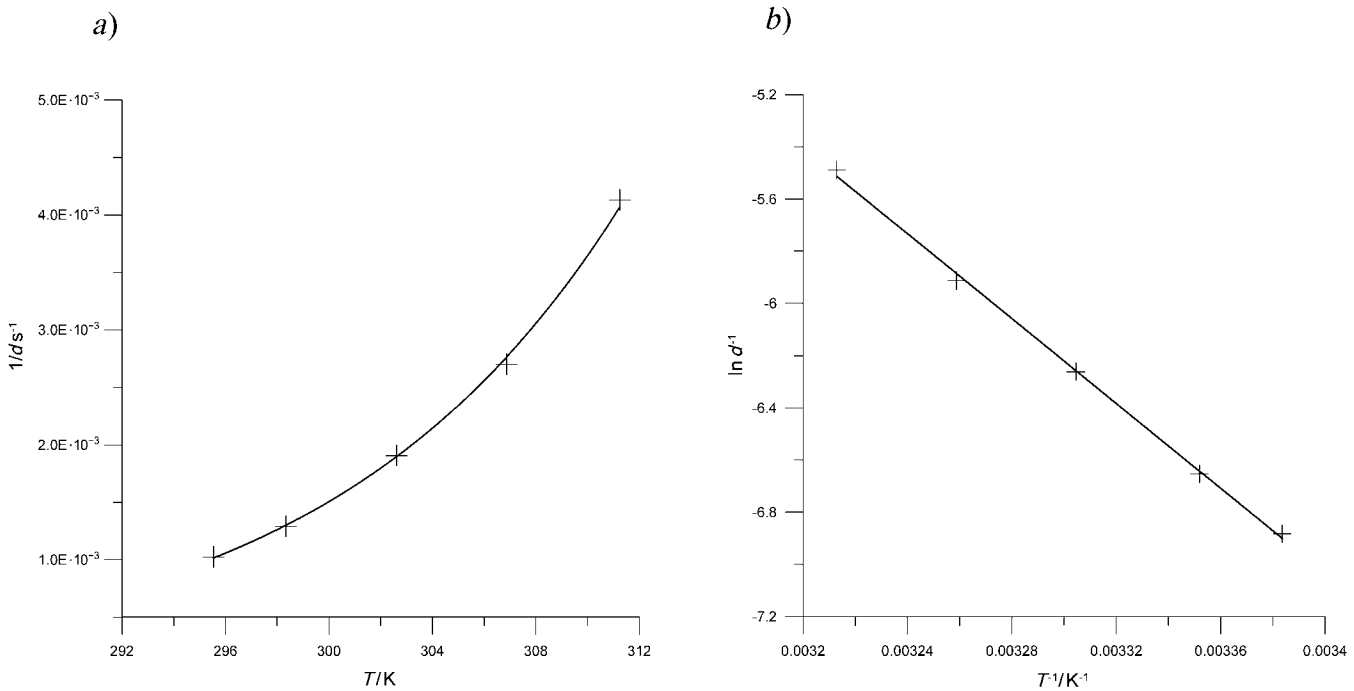

Fig. 10. a) *The inverse 1*/d *of the duration of oscillations plotted as a function of* T [K] (initial composition of the mixture, see text). b) *Plot of ln(1*/d*)* vs. *1*/T.

Table 5. *Apparent 'Average Activation Energies'*

Antioxidant	Antioxidant added to mixture [mol l^{-1}]	E_{t_i} during the inhibition time [kJ]	E_{d_r} after the restart of oscillations [kJ]
ferulic acid	$1.66 \cdot 10^{-6}$	90 ± 4	94 ± 6
Isoferulic acid	$1.66 \cdot 10^{-6}$	75 ± 3	72 ± 3
Caffeic acid	$1.79 \cdot 10^{-6}$	70 ± 2	74 ± 2
2,5-DHBA	$2.09 \cdot 10^{-5}$	64 ± 2	91 ± 4

errors, leads to the following observations and conclusions: *i*) The apparent 'average activation energies' for the resumed oscillatory phase (E_{d_r}) are significantly different from that of the uninhibited reaction (E_{av}). This seems to confirm that the restarting of the oscillations is caused by different substrates than malonic acid, probably products of the degradation of the ArO$^{\cdot}$ radicals. Indeed, the amplitude and the time length of the resumed oscillations are different from those of the uninhibited oscillating system. It must also be considered that, at high concentrations of the antioxidant added, the amplitude of the resumed oscillations becomes too low, so that, at a given concentration (different for each antioxidant), oscillations do not restart. This means that the oscillating reaction reached its end, having been unable to produce radicals. Presumably most of the malonic acid is decomposed during the inhibition phase.

ii) At the concentrations of the antioxidants added, there is no doubt that, for ferulic and isoferulic acid, the inhibition phase is characterized by reactions different from those of the chain reactions that lead to the oscillations. For these compounds, the 'average activation energy' of the inhibition phase (E_{t_i}) is significantly different than that of the uninhibited reaction (E_{av}). This fact is less evident for caffeic acid and 2,5-DHBA. Within the experimental errors, the E_{t_i} values are not significantly different from the E_{av} value of the uninhibited reaction.

4. Some Final Remarks. – The results of both experimental and mechanistic work clearly show that, in the inhibitory phase, other reactions besides H-atom transfer from diphenols (= benzenediol derivatives) to HOO$^{\cdot}$ radicals can occur. Thus, parallel reactions of oxidation and/or iodination of the antioxidants by IO_3^- and I_2 are possible during quenching of oscillations in the *BR* system. However, both quinones and iodinated products deplete HOO$^{\cdot}$ radicals, so we can conclude that the main action of diphenols is quenching of the radicals. Therefore, the oscillating *BR* reaction is suitable as an analytical method to measure relative activities of antioxidant scavengers of free radicals. However, attention must be paid to the order of addition of reactants, *i.e.*, malonic acid, $MnSO_4$, $HClO_4$, $NaIO_3$, and H_2O_2. Oscillations start after the addition of H_2O_2. Generally, 1.00 ml of a suitably diluted solution of antioxidant is added after the third oscillation. According to this sequence, the measured inhibition times are highly reproducible and can be used for relative antioxidant-activity calculations [1][5].

The ranking order of antioxidant capacity measured with the *BR* method for some diphenols [1] is in satisfactory agreement with that obtained with the TEAC (trolox equivalent antioxidant capacity) method [14], taking into account that this latter works at pH 7.4. Finally, the method based on the *Briggs–Rauscher* oscillating reaction makes

it possible to determine the activity of antioxidants at low pH, which was difficult prior to the advent of this method.

REFERENCES

[1] R. Cervellati, K. Höner, S. D. Furrow, C. Neddens, S. Costa, *Helv. Chim. Acta* **2001**, *84*, 3533.
[2] T. S. Briggs, W. C. Rauscher, *J. Chem. Educ*. **1973**, *50*, 496.
[3] K. Höner, R. Cervellati, C. Neddens, *Eur. Food Res. Technol*. **2002**, *214*, 356.
[4] K. Höner, R. Cervellati, *Eur. Food Res. Technol*. **2002**, *215*, 437.
[5] R. Cervellati, C. Renzulli, M. C. Guerra, E. Speroni, *J. Agric. Food Chem*. **2002**, *50*, 7504; also mentioned in *Gastroenterology Week* **2003**, February 17 issue.
[6] R. Cervellati, N. Crespi-Perellino, S. D. Furrow, A. Minghetti, *Helv. Chim. Acta* **2000**, *83*, 3179.
[7] S. D. Furrow, R. Cervellati, G. Amadori, *J. Phys. Chem. A* **2002**, *106*, 5841.
[8] R. M. Noyes, S. D. Furrow, *J. Am. Chem. Soc*. **1982**, *104*, 45.
[9] 'Gepasi Program', free download at http://gepasi.dbs.aber.ac.uk/softw/gepasi.html; P. Mendes, *Comput. Appl. Biosci*. **1993**, *9*, 563; P. Mendes, *Trends Biochem. Sci*. **1997**, *22*, 361; P. Mendes, D. B. Kell, *Bioinformatics* **1998**, *14*, 869.
[10] A. J. Bard, R. Parson, J. Jordan, 'Standard Potentials in Aqueous Solution', Marcel Dekker Inc., New York and Basel, 1985, Chapt. 4.
[11] R. Cervellati, P. Fetto, G. Dalbagni, *Educ. Chem*. **1998**, *35*, 50.
[12] R. Cervellati, S. D. Furrow, S. De Pompeis, *Int. J. Chem. Kinet*. **2002**, *34*, 357.
[13] R. Ramaswami, N. Ganapathisubramanian, *J. Chem. Educ*. **1979**, *56*, 321.
[14] N. J. Miller, C. A. Rice-Evans, M. J. Davies, V. Gopinathan, *Clin. Sci*. **1993**, *84*, 407.

Received July 7, 2003